Anales de Mecánica de la Fractura

TEXTO DE LAS COMUNICACIONES PRESENTADAS EN EL

1st VIRTUAL IBERIAN CONFERENCE ON STRUCTURAL INTEGRITY

Número 37

25, 26 y 27 de marzo de 2020

Anales de Mecánica de la Fractura

Texto de las comunicaciones presentadas en el

1st Virtual Iberian Conference on Structural Integrity

25, 26 y 27 de marzo de 2020

Editado por la Secretaría del Grupo Español de Fractura

I.S.S.N.: 0213-3725
Fecha publicación: diciembre 2020

EDITORIAL

El volumen 37 de los Anales de Mecánica de la Fractura incluye las comunicaciones presentadas en la 1st Virtual Iberian Conference on Structural Integrity. Esta primera edición virtual sustituye a la 5th Iberian Conference on Structural Integrity que, en principio, se iba a celebrar en Coimbra el 25, 26 y 27 de marzo del 2020, y que tuvo que ser suspendido debido a la situación mundial de la pandemia generada por el COVID-19. En esta ocasión, la organización del congreso, promovido por la Sociedad Portuguesa de Integridad Estructural y el Grupo Español de Fractura – Sociedad Española de Integridad Estructural, ha recaído en la Universidad de Coimbra y en el Politécnico de Coimbra.

Los congresos ibéricos o hispano-portugueses se han celebrado en cuatro ocasiones: Braga (1987), Mérida (1993), Luso (1996) y Porto (2010). Y han sido un foro de encuentro de investigadores y profesionales interesados en la integridad de materiales y estructuras, contituyendo el marco ideal para mostrar avances e intercambiar ideas entre los investigadores de España y Portugal.

Deseamos agradecer el trabajo y el esfuerzo de todos los autores que han hecho posible la edición de este volumen asociado a la primera conferencia virtual con un total de 57 trabajos.

También expresamos nuestro agradecimiento a los miembros del Comité Científico, quienes han participado activamente en la organización de la conferencia.
En diciembre de 2020

El Comité Organizador

EDITORIAL

Volume 37 of the Annals of Fracture Mechanics includes the communications presented at the I Iberian Virtual Congress on Structural Integrity. This first virtual edition has been launched since the 5th Iberian Conference on Structural Integrity which, in principle, would be held in Coimbra on March 25, 26 and 27, 2020 had to be postponed to 2021 due to the global situation of the pandemic generated by COVID-19. On this occasion, the organization of the congress promoted by the Portuguese Society of Structural Integrity and the Spanish Group of Fracture - Spanish Society of Structural Integrity has fallen to the University of Coimbra and the Polytechnic of Coimbra.

Iberian or Spanish-Portuguese congresses have been held on four occasions: Braga (1987), Mérida (1993), Luso (1996) and Porto (2010). And they have been a meeting forum for researchers and professionals interested in the integrity of materials and structures, being the opportunity to show progress and exchange ideas between researchers from Spain and Portugal.

We wish to thank the work and effort of all the authors who have made possible the edition of this volume associated with the first virtual conference with a total of 57 papers.

We also wish to thank the members of the Scientific Committee, who have actively participated in the organization.

December 2020

The Organizing Committee

Junta Directiva de la Sociedad Española de Integridad Estructural – Grupo Español de Fractura (SEIE-GEF)

Presidente:	Francisco Gálvez Díaz-Rubio (Universidad Politécnica de Madrid)
Vicepresidente 1º:	Jesús Manuel Alegre Calderón (Universidad de Burgos)
Vicepresidente 2º:	Eugenio Giner Maravilla (Universidad de Valencia)
Vicepresidente 3º:	Cristina Rodríguez González (Universidad de Oviedo)
Vicepresidente 4º:	Carlos Navarro Pintado (Universidad de Sevilla)
Vicepresidente 5º:	Orlando Santana Pérez (Universidad Politécnica de Cataluña)
Secretaria:	Alicia Salazar López (Universidad Rey Juan Carlos)
Tesorero:	Luis Távara Mendoza (Universidad de Sevilla)

Organizadores del 1st Virtual Iberian Conference on Structural Integrity

Presidentes del Comité Organizador

Luís Filipe Borrego

José Martins Ferreira

Comité Organizador

José Domingos Costa

Pedro Moreira

Virgínia Infante

Fernando Ventura Antunes

Ricardo Branco

Comité Científico

Abílio de Jesus
(Universidade do Porto)

Alfredo da Silva Ribeiro
(Universidade de Trás-os-Montes e Alto Douro)

Andrés Valiente Cancho
(Universidad Politécnica de Madrid)

António Mário Henriques Pereira
(Escola Superior de Tecnologia e Gestão de Leiria)

Alfonso Fernández Canteli
(Universidad de Oviedo)

Alicia Salazar López
(Universidad Rey Juan Carlos)

António Augusto Fernandes
(Universidade do Porto)

Antonio Martín Meizoso
(Universidad de Navarra, CEIT)

Armando Ramalho
(Politécnico de Castelo Branco)
Carlos Capela
(Escola Superior de Tecnologia e Gestão de Leiria)
Carmen Baudín
(Instituto de Cerámica y vidrio, CSIC)
Emilio García Pañeda
(Imperial College London)
Fernando Ventura Antunes
(Universidade de Coimbra)
Francisco Gálvez Díaz-Rubio
(Universidad Politécnica de Madrid)
Idoia Urrutibeascoa
(Universidad de Mondragón)
Jaime Planas Roselló
(Universidad Politécnica de Madrid)
Jesús Manuel Alegre Calderón (Universidad de Burgos)
José Alberto Álvarez Laso
Universidad de Cantabria)
José Cardoso Xavier
(Universidade Nova de Lisboa)
José Fernández Sáez
(Universidad Carlos III de Madrid)

Luís F. G. Reis
(Instituto Superior Técnico)

Luís Roseiro
(Instituto Superior de Engenharia de Coimbra)
Mª Lluisa Maspoch
Universidad Politécnica de Cataluña)
Manuel Moreira de Freitas
(Instituto Superior Técnico)
Paulo Nobre dos Reis
(Universidade da Beira Interior)

Paulo Tavares (INEGI)

Pedro Moreira (INEGI)

Belen Moreno
(Universidad de Málaga)

Carlos Navarro Pintado
(Universidad de Sevilla)

Cristina Rodríguez González
(Universidad de Oviedo)
Eugenio Giner Maravilla
(Universidad Politécnica de Valencia)
Filipe Samuel Silva
(Universidade do Minho)
Gonzalo Ruíz López
(Universidad de Castilla - La Mancha)
Jaime Domínguez Abascal
(Universidad de Sevilla)

Javier Belzunce (Universidad de Oviedo)

Jesús Toribio Quevedo
(Universidad de Salamanca)
José António Correia
(Universidade do Porto)
José Domingos Costa
(Universidade de Coimbra)
José Martins Ferreira
(Universidade de Coimbra)
Luís Filipe Borrego
(Instituto Superior de Engenharia de Coimbra)
Luis Távara Mendoza
(Universidad de Sevilla)
Manuel Fonte
(Escola Superior Náutica)
Orlando Santana Pérez
(Universidad Politécnica de Cataluña)
Paulo Tavares de Castro
(Universidade do Porto)
Pedro Bravo Díez
(Universidad de Burgos)
Ricardo Batista
(Instituto Politécnico de Setúbal)

Ricardo Branco
(Universidade de Coimbra)
Rui F. Martins
(Universidade Nova de Lisboa)
Virgínia Infante (Instituto Superior Técnico)

Ricardo Cláudio
(Instituto Politécnico de Setúbal)
Sergio Cicero González
(Universidad de Cantabria)

Patrocinadores

ÍNDICE

NUMERICAL STUDY ON THE PLASTIC STRAIN GENERATED DURING THE SLM PROCESS

D.M. Neto[1*], C.M. Andrade[1], M.C. Oliveira[1], J.L. Alves[2], L.F. Menezes[1]

[1] University of Coimbra, CEMMPRE, Department of Mechanical Engineering,
Rua Luís Reis Santos, Pinhal de Marrocos, 3030-788 Coimbra, Portugal
[2] CMEMS, Microelectromechanical Systems Research Unit, University of Minho,
Campus de Azurém, 4800-058 Guimarães, Portugal
[*] Contact person: diogo.neto@dem.uc.pt

RESUMEN

Las piezas producidas por fusión selectiva por láser (SLM) sufren una distorsión permanente no deseada, asociada con los altos niveles de estrés residual. La simulación numérica puede ser extremadamente valiosa, ya que es imposible evaluar experimentalmente el estado de tensión total. Para reducir el costo computacional es común adoptar estrategias multiescala, como el método de deformación inherente, donde el campo de deformación plástica se mapea capa por capa para la simulación de la pieza completa. Este estudio presenta la simulación termomecánica de un proceso de deposición de una sola capa, que permite evaluar tanto el estado de la tensión residual como el campo de deformación plástica generado por los ciclos térmicos. El modelo de elementos finitos propuesto considera el acoplamiento del problema de conducción de calor transitorio con el análisis mecánico elástico/perfectamente plástico. Como el proceso SLM comprende los fenómenos de fusión, solidificación y enfriamiento, el modelo considera los cambios de fase polvo-líquido-sólido, que se establecen cambiando las propiedades del material. Además, se asume que las propiedades térmicas y mecánicas del material dependen de la temperatura. Los resultados muestran que el proceso de deposición induce tensiones plásticas no despreciables en la interfaz entre las capas.

PALABRAS CLAVE: Fabricación aditiva; Fusión selectiva por láser; Modelación termomecánica; Campo de deformación plástica

ABSTRACT

Parts produced by selective laser melting (SLM) experience unwanted permanent distortion which has been associated with high levels of residual stress. The numerical simulation can be extremely valuable, since the full stress state is impossible to evaluate experimentally. In order to reduce the computational cost, some multi-scale strategies have been adopted, namely the inherent strain method, where the plastic strain field is mapped layer-by-layer to the simulation of the full part. This study presents the thermomechanical simulation of a single-track deposition process, allowing to evaluate both the residual stress state and the plastic strain field generated by the thermal cycles. The proposed finite element model considers the coupling of the transient heat conduction problem with the mechanical elastic/perfectly-plastic analysis. Since the SLM process comprises the melting, solidification and cooling phenomena, the model considers the powder-liquid-solid phase changes, which is established by changing the material properties. Besides, both the thermal and mechanical material properties are assumed as temperature dependent. The results show that the deposition process induces non-negligible plastic strains at the interface between the layers.

KEYWORDS: Additive manufacturing; Selective laser melting; Thermo-mechanical modelling; Plastic strain field

INTRODUCTION

Metal powder based additive manufacturing (AM) technologies have been growing in importance in the last years due to their unique features that are revolutionizing multiple industrial fields. The Selective Laser Melting (SLM) process is one of the most relevant in the manufacture of metallic parts using AM. This technology has grown exponentially in the automotive and aeronautic industries due to the great potential to create highly complex and customized parts, with geometric designs that are impossible to produce with traditional (subtractive) processes [1]. In this process, a laser beam is used to melt predefined regions of a layer of powder, according to the information provided by a CAD model. Then, another layer of powder is added and the laser scans again. This is successively repeated until the complete part is built (layer-by-layer fabrication). The moving heat source leads to heating, melting and solidification of the metallic alloy, creating repeated heating and cooling cycles on the work piece [2]. The large temperature gradients generated during this process and the non-uniform thermal expansions and contractions in the heat affected zone result in the formation of inhomogeneous plastic deformation [3]. This is responsible for high residual stresses in the finished part, whose magnitude

can exceed the yield strength of the alloy [4]. Consequently, the dimensional accuracy (particularly in thin-walled features) and mechanical performance of the parts can be compromised [5]. In fact, one of the current main challenges of AM processes is the incapability to predict the end-use mechanical properties of the built parts, determined by the final microstructure and porosity [6].

Due to the complexity of the physical phenomena associated to the SLM process and the influence of numerous process parameters in the quality of the final built parts, an experimental trial-and-error approach to optimize the process is prohibitively expensive. Therefore, numerical simulation assumes a critical role for understanding the characteristics of the SLM process, as well as better predicting the final part properties and creating guidelines for the optimization of the manufacturing process. Nevertheless, the multi-physics and multi-scale nature of this AM process represents a big challenge for numerical simulation tools. There are three scales for SLM numerical modelling: micro-scale, meso-scale and macro-scale. The micro-scale models focus in the melt pool dynamics, comprising the interaction between the laser beam and the powder particles, heat transfer, phase change, capillary and Marangoni forces, evaporation pressure and wetting [7]. The computational cost of this type of analysis tends to be very high, particularly when more effects are included. The meso-scale models are dedicated to the modelling of sub-regions of the process, comprising the interactions between the laser beam and the powder bed, which is considered as a continuum with a certain percentage of porosity. This approach usually considers a given number of laser scans over a series of layers (small volume element representative of the whole part) and can predict the residual stress distribution within that region. Finally, the macro-scale is used to obtain temperature fields and distributions of distortions and residual stresses at the part scale. For this approach a number of simplifications have to be made to reduce the complexity of the physical phenomena that occur at the smaller scales [3]. Recently, several computational tools that combine the macro-scale [8] with meso-scale [9] and multi-scale modelling [10] have been developed. These are based on the knowledge that the interaction between thermal and mechanical responses requires the development of robust thermo-mechanical coupling models. In fact, the accurate prediction of the plastic strain field, residual stresses and part distortions requires an accurate temperature field estimation, for each step the whole process.

Since an effective analysis of the SLM process requires the adoption of macro-scale models, the finite element method is typically used to predict the transient temperature distribution in the parts obtained by SLM. Then, using the obtained temperature field, the thermal stress field and the residual stresses can be estimated by a thermo-mechanical coupling model [11]. However, this process involves large temperature changes, which leads to strong variations of the thermo-mechanical properties and, consequently, generates a nonlinear problem, which leads to the increase of the computation cost. Therefore, although the SLM process is inherently multi-layer, most of the studies are focused on single layer deposition [12]. This simplification neglects the inter-layer thermal interactions, affecting the precision of the predicted plastic strain field, but allows a drastic reduction of the computational effort. The main goal of this study is to assess the plastic strain field generated in a single-track deposition. Accordingly, the thermo-mechanical analysis of a small volume representative of the whole part is carried out to find the evolution of the temperature induced stress and strain state. The stainless steel 316L is adopted in the present study, considering temperature dependent material properties.

THERMO-MECHANICAL MODEL

In the present study, the numerical analysis of the SLM process is carried out using a 3D thermo-mechanical modelling approach, based on the staggered coupling proposed in [13]. This approach evaluates the transient thermal problem and the thermo-elasto-plastic behaviour of the component, solved sequentially in each time increment.

2.1. Heat transfer modelling

The differential equation governing the transient heat conduction within a continuous medium with arbitrary volume can be derived from the first law of thermodynamics and is expressed as follows:

$$k\left(\frac{\partial^2 T}{\partial x^2}+\frac{\partial^2 T}{\partial y^2}+\frac{\partial^2 T}{\partial z^2}\right)+\dot{q}=\rho c_{\mathrm{p}}\frac{\partial T}{\partial t}, \qquad (1)$$

where k is the thermal conductivity coefficient, ρ denotes the mass density, c_{p} is the specific heat and $\dot{q}$ is the power generated per volume in the workpiece. The solution of the heat equation provides the evolution of the temperature T with respect to time t, for each material point.

Due to the porosity in the powder bed, the incident laser radiation is reflected between the particles, increasing the absorption depth in comparison to the one observed for the bulk solid [14]. Thus, the laser heat input is modelled by the volumetric Gaussian heat source proposed by Goldak [15]. The power density distribution for a hemispherical shape heat source model can be expressed as:

$$\dot{q}=\frac{2^{5/2}\beta P}{\pi^{3/2} r_0^{\,3}}\exp\left\{-2\frac{x^2+y^2+z^2}{r_0^{\,2}}\right\}, \qquad (2)$$

where P is the power of the laser source, β is the absorptivity of the laser beam and r_0 denotes the radius of the laser beam.

2.2. Mechanical modelling

The *quasi*-static mechanical analysis of the workpiece is carried out taking into account the predicted temperature field, which affects the mechanical response. The balance of linear momentum in any point of the body (part to be manufactured) is given by:

$$\mathrm{div}(\boldsymbol{\sigma}) + \mathbf{b} = \mathbf{0}\,, \tag{3}$$

where $\boldsymbol{\sigma}$ is the stress tensor and $\mathbf{b}$ are the body forces, which are neglected in the present model. Regarding the boundary conditions, prescribed displacements are imposed on the Dirichlet boundary. In this study, the substrate bottom is assumed as being fixed, both during the SLM processing as well as during the cooling stage.

The total strain increment is the superposition of the following terms:

$$\Delta\boldsymbol{\varepsilon}^{\mathrm{total}} = \Delta\boldsymbol{\varepsilon}^{\mathrm{e}} + \Delta\boldsymbol{\varepsilon}^{\mathrm{p}} + \Delta\boldsymbol{\varepsilon}^{\mathrm{th}}\,, \tag{4}$$

where $\Delta\boldsymbol{\varepsilon}^{\mathrm{e}}$ is the elastic strain increment, $\Delta\boldsymbol{\varepsilon}^{\mathrm{p}}$ is the plastic strain increment and $\Delta\boldsymbol{\varepsilon}^{\mathrm{th}}$ is the thermal strain increment. The effects of strains induced by solid-state phase transformation and creep are neglected in the present model. The Hooke's elastic constitutive law defines the linear relationship between the stress tensor and the elastic strain tensor as follows:

$$\boldsymbol{\sigma}^{\mathrm{e}} = \mathbf{C} : \boldsymbol{\varepsilon}^{\mathrm{e}}\,, \tag{5}$$

where $\mathbf{C}$ is the fourth-order material stiffness tensor. Assuming an isotropic linear elastic material, the stiffness matrix $\mathbf{C}$ can be calculated from the Young's modulus (E) and the Poisson's ratio (ν), which can be both temperature dependent. Considering an associated flow rule in the plasticity model, the plastic strain increment is given by:

$$\Delta\boldsymbol{\varepsilon}^{\mathrm{p}} = \Delta\lambda\frac{\partial f}{\partial\boldsymbol{\sigma}}\,, \tag{6}$$

where $\Delta\lambda$ is the increment of the plastic multiplier, which is calculated through the consistency condition. The plastic behaviour is also assumed as isotropic, described by the von Mises yield criterion. Hence the yield function f is defined as follows:

$$f = \sigma_{\mathrm{vM}} - \sigma_{\mathrm{y}} \le 0\,, \tag{7}$$

where σ_{vM} represents the von Mises equivalent stress and σ_{y} is the yield stress. The perfectly-plastic model is adopted, i.e. the hardening behaviour of the material is neglected. Hence, the temperature dependent values of σ_{y} follow the initial yield stress σ_0. The total thermal strain is calculated as:

$$\boldsymbol{\varepsilon}^{\mathrm{th}} = \left(\alpha_T(T - T_{\mathrm{ref}}) - \alpha_{\mathrm{ini}}(T_{\mathrm{ini}} - T_{\mathrm{ref}})\right)\mathbf{I}\,, \tag{8}$$

where α_T and α_{ini} are the volumetric thermal expansion coefficients evaluated at the current temperature T and at the initial temperature T_{ini}, respectively. T_{ref} is the reference temperature used to define the thermal expansion coefficients and $\mathbf{I}$ denotes the second-order identity tensor.

FINITE ELEMENT MODEL

The numerical simulations were carried out with the in-house finite element code DD3IMP, originally developed to simulate sheet metal forming processes [16]. The solution of the transient heat conduction problem is obtained using the Euler's backward method [17], while the evolution of the deformation is described by an updated Lagrangian scheme. Both the thermal and the mechanical problems use the same finite element mesh (linear hexahedral elements). However, full integration is adopted in the thermal problem, while the mechanical problem uses the selective reduced integration technique [18] to avoid volumetric locking.

3.1. SLM process conditions

In order to reduce the computational cost associated with the numerical simulation, the domain considered for the SLM process was significantly decreased. Thus, only a single-track deposition was studied, which was assumed to be scanned over consolidate layers. Moreover, the finite element model considers 2D conditions, simulating only the vertical plane containing the laser path. The geometry of the initial domain is presented in Figure 1, including dimensions. All domain is composed by the same material: stainless steel 316L. The domain of the powder bed above the solidified layers (40 μm of thickness) presents a uniform finite element mesh with 10 μm of edge size.

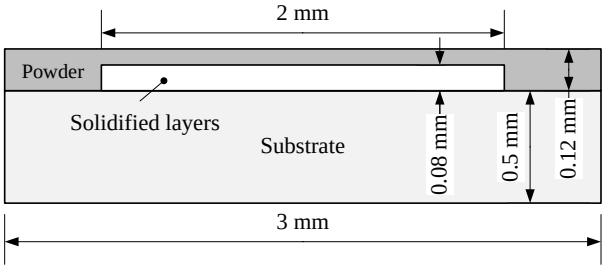

Figure 1. Geometry of the initial solution domain used in the thermo-mechanical analysis of the SLM process.

Since the substrate is considered to be preheated at 200ºC, the initial temperature of the system (substrate, solidified layers and powder bed) is assigned with this value. The proposed model considers the heat loss by convection/radiation between the upper surface of the powder and the environment. The heat convection coefficient was set to 100 W/m^{2}K according to [20], which takes into account also heat loss due to radiation, while the environment temperature is assumed constant during the SLM process (set to 200ºC). Regarding the process parameters considered in the numerical simulations, specifically the ones involved in Eq. (3) to describe the laser beam, the power is assumed equal to 50 W, the spot radius is 50 μm and the absorptivity of the powder material is 0.3 [12]. Since the adopted scanning speed is 600 mm/s, the processing time is 3.17 ms.

3.2. Thermo-mechanical material properties

Since the SLM process comprises the material phase transformation from powder to liquid, which then cools down to solidification, three material phases were considered in the simulation: powder, solid and liquid. Each material phase requires a set of temperature dependent material properties, which are listed in Table 1. The thermo-physical properties were obtained from [21], while the mechanical properties were extracted from [12]. The melting point of the stainless steel 316L is 1450ºC, according to [21], which is indicated in Table 1 by the dashed line, separating the properties of the solid material (bulk) from the liquid phase. Both the thermal expansion coefficient and the Poisson's ratio are assumed temperature independent, adopting the values of 20×10^{-6} K^{-1} and 0.3, respectively.

Table 1. Temperature dependent material properties for solid and liquid stainless steel 316L.

T [ºC]	ρ [kg/m^3]	c_p [J/kg·K]	k [W/m·K]	E [GPa]	σ_0 [MPa]
25	7950	470	13.4	198.5	282
600	7681	590	24.5	157	153
700	7628	600	25.1	141	108
800	7575	630	27.2	106	50
1300	7311	710	31.1	10	5
1450	7236	730	29.8	0.05	2.5
1500	6842	830	100	0.05	
1600	6765	830	100	0.05	

The thermal conductivity coefficient of the liquid phase was artificially increased (see Table 1) to account for the strong convective heat transfer within the melt pool. Besides, the mechanical strength of the liquid is considered very weak and the thermal expansion is ignored. Considering a value of 0.6 for the packing factor of the powder bed, the mass density of the powder phase is 60% of the solid. On the other hand, the specific heat of the powder phase is 50% of the solid accordingly to [22], while the thermal conductivity coefficient is 1% of the solid. The mechanical strength of the powder material is assumed weak, but the thermal expansion coefficient is assumed identical to the one adopted for the solid material.

RESULTS AND DISCUSSION

The thermal history of each finite element is used to define the material phase status, using the melting temperature as bound. Accordingly, the assigned material phase (powder, solid and liquid) is presented in Figure 2 (a) for the instant corresponding to the end of the laser scanning phase. The predicted temperature field is presented in Figure 2 (b) for the same instant, highlighting the strong temperature gradient near the laser beam. The predicted distribution for the von Mises equivalent stress in the built component is presented in Figure 2 (c), which is largest in the region of the substrate. The predicted plastic strain is presented in Figure 2 (c) for the same instant, highlighting that the large value of plastic strain occurs in the interface between the solidified layers and the deposited one.

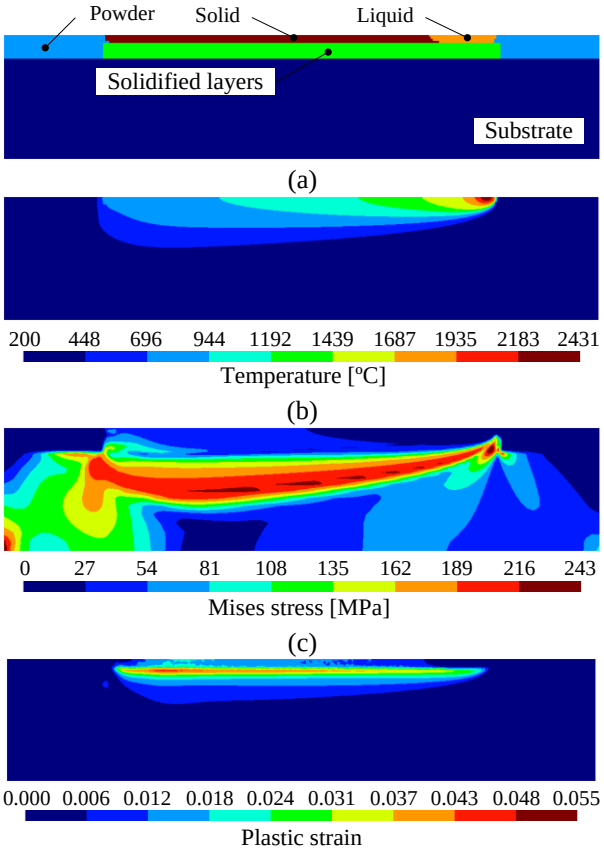

Figure 2. Predicted results after laser scanning: (a) assigned material phase; (b) temperature distribution; (c) von Mises stress distribution; (d) plastic strain distribution.

Since the temperature after the laser scanning is significantly higher than the environment temperature (200ºC), both the stress and the strain are influenced by

the cooling time. As shown in Figure 3 (a), after 0.5 s of cooling, the liquid phase vanishes, due to the heat losses with the environment. Accordingly, the predicted temperature field presented in Figure 3 (b) shows an approximately uniform distribution over the entire domain. The predicted distribution for the von Mises equivalent stress in the component is presented in Figure 3 (c). Since the temperature decreased significantly in the region of the deposited layer (in comparison with the instant after laser scanning), the equivalent stress increased in this region. Nevertheless, it is more uniform after cooling since the temperature gradient vanished. The predicted plastic strain is presented in Figure 3 (c) for the same instant. The results highlight that the value of plastic strain increases during the cooling down. Indeed, the maximum predicted plastic strain in the current deposited layer is about 3%, which increases to around 5% at the interface between the current layer and the preceding deposited layers.

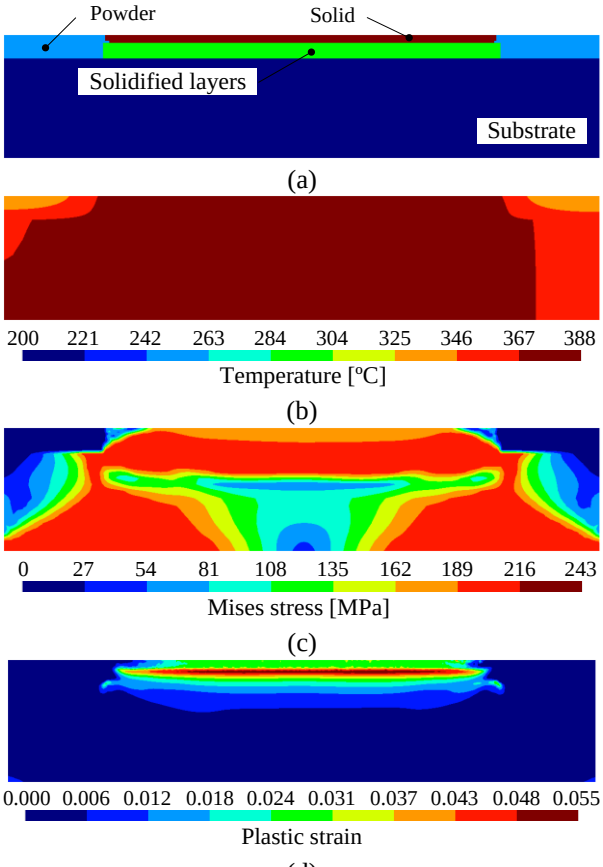

Figure 3. Predicted results after 0.5 s of cooling time: (a) assigned material phase; (b) temperature distribution; (c) von Mises stress distribution; (d) plastic strain distribution.

CONCLUSIONS

This study presents the thermo-mechanical analysis of a single-track deposition during an SLM process. The proposed 2D model comprises the transient thermal behaviour and the elastic/perfectly-plastic mechanical behaviour. In order to accurately predict the coupling between the transient temperature history and the mechanical response, both the thermal and mechanical material properties are assumed as temperature dependent. The dimension of the melt pool is estimated based on the predicted temperature distribution, which is mainly dictated by the heat conduction mechanism. The stainless steel 316L is adopted in this study to assess the influence of the process conditions on plastic strain. The residual stresses in the finished part are consequence of the material thermal expansion, together with the severe temperature gradients. After cooling down, the plastic strain in the current deposited layer is about 3%, which increases to around 5% at the interface between the current layer and the preceding deposited layers. These results confirm that the level of plastic strain induced by a single-track deposition cannot be neglected when estimating the residual stress in a SLM part.

ACKNOWLEDGMENTS

This research work was sponsored by national funds from the Portuguese Foundation for Science and Technology (FCT) under the project with reference PTDC/EME-EME/31657/2017 and by European Regional Development Fund (ERDF) through the Portugal 2020 program and the Centro 2020 Regional Operational Programme (CENTRO-01-0145-FEDER-031657) under the project MATIS (CENTRO-01-0145-FEDER-000014) and UID/EMS/00285/2020.

REFERENCES

[1] C. Tan, K. Zhou, W. Ma, B. Attard, P. Zhang, T. Kuang, Selective laser melting of high-performance pure tungsten: parameter design, densification behavior and mechanical properties, Sci. Technol. Adv. Mater., 19 (2018) 370–380.

[2] W.J. Sames, F.A. List, S. Pannala, R.R. Dehoff, S.S. Babu, The metallurgy and processing science of metal additive manufacturing, Int. Mater. Rev., 61 (2016) 315–360.

[3] L.A. Parry, Investigation of Residual Stress in Selective Laser Melting, PhD Thesis, University of Nottingham, 2017.

[4] T. Mukherjee, W. Zhang, T. DebRoy, An improved prediction of residual stresses and distortion in additive manufacturing, Comput. Mater. Sci., 126 (2017) 360–372.

[5] S. Das, Physical Aspects of Process Control in Selective Laser Sintering of Metals, Adv. Eng. Mater., 5 (2003) 701–711.

[6] Y. Zhang, G. Guillemot, M. Bernacki, M. Bellet, Macroscopic thermal finite element modeling of additive metal manufacturing by selective laser melting process, Comput. Methods Appl. Mech. Eng., 331 (2018) 514–535.

[7] M. Markl, C. Körner, Multiscale Modeling of Powder Bed–Based Additive Manufacturing, Annu. Rev. Mater. Res., 46 (2016) 93–123.

[8] D. Riedlbauer, T. Scharowsky, R.F. Singer, P. Steinmann, C. Körner, J. Mergheim, Macroscopic simulation and experimental measurement of melt pool characteristics in selective electron beam melting of Ti-6Al-4V, Int. J. Adv. Manuf. Technol., 88 (2017) 1309–1317.

[9] C. Panwisawas, C. Qiu, M.J. Anderson, Y. Sovani, R.P. Turner, M.M. Attallah, J.W. Brooks, H.C. Basoalto, Mesoscale modelling of selective laser melting: Thermal fluid dynamics and microstructural evolution, Comput. Mater. Sci., 126 (2017) 479–490.

[10] C. Li, C.H. Fu, Y.B. Guo, F.Z. Fang, A multiscale modeling approach for fast prediction of part distortion in selective laser melting, J. Mater. Process. Technol., 229 (2016) 703–712.

[11] L. Parry, I.A. Ashcroft, R.D. Wildman, Understanding the effect of laser scan strategy on residual stress in selective laser melting through thermo-mechanical simulation, Addit. Manuf., 12 (2016) 1–15.

[12] A. Hussein, L. Hao, C. Yan, R. Everson, Finite element simulation of the temperature and stress fields in single layers built without-support in selective laser melting, Mater. Des., 52 (2013) 638–647.

[13] J.M.P. Martins, D.M. Neto, J.L. Alves, M.C. Oliveira, H. Laurent, A. Andrade-Campos, L.F. Menezes, A new staggered algorithm for thermomechanical coupled problems, Int. J. Solids Struct., 122–123 (2017) 42–58.

[14] J.F. Li, L. Li, F.H. Stott, Comparison of volumetric and surface heating sources in the modeling of laser melting of ceramic materials, Int. J. Heat Mass Transf., 47 (2004) 1159–1174.

[15] J. Goldak, A. Chakravarti, M. Bibby, A new finite element model for welding heat sources, Metall. Trans. B, 15 (1984) 299–305.

[16] L.F. Menezes, C. Teodosiu, Three-dimensional numerical simulation of the deep-drawing process using solid finite elements, J. Mater. Process. Technol., 97 (2000) 100–106.

[17] J.M.P. Martins, J.L. Alves, D.M. Neto, M.C. Oliveira, L.F. Menezes, Numerical analysis of different heating systems for warm sheet metal forming, Int. J. Adv. Manuf. Technol., 83 (2016) 897–909.

[18] T.J.R. Hughes, Generalization of selective integration procedures to anisotropic and nonlinear media, Int. J. Numer. Methods Eng., 15 (1980) 1413–1418.

[19] Y.P. Yang, M. Jamshidinia, P. Boulware, S.M. Kelly, Prediction of microstructure, residual stress, and deformation in laser powder bed fusion process, Comput. Mech., 61 (2018) 599–615.

[20] H.-S. Tran, J.T. Tchuindjang, H. Paydas, A. Mertens, R.T. Jardin, L. Duchêne, R. Carrus, J. Lecomte-Beckers, A.M. Habraken, 3D thermal finite element analysis of laser cladding processed Ti-6Al-4V part with microstructural correlations, Mater. Des., 128 (2017) 130–142.

[21] K.C. Mills, Recommended values of thermophysical properties for selected commercial alloys, Woodhead Publishing Limited, 2002.

[22] N.E. Hodge, R.M. Ferencz, J.M. Solberg, Implementation of a thermomechanical model for the simulation of selective laser melting, Comput. Mech., 54 (2014) 33–51.